

Steady-state flow model of debris-covered glaciers (rock glaciers)

SARAH K. KONRAD & NEIL F. HUMPHREY

*Department of Geology and Geophysics, University of Wyoming, PO Box 3006, Laramie,
Wyoming 82071, USA*

e-mail: skon@uwyo.edu

Abstract A two-dimensional, steady-state, flow line model of a debris-covered glacier is developed using mass conservation of debris and ice. Ice deformation is driven by shear stress, estimated from the local ice and debris overburden. Input variables are altitude-dependant ice mass balance, debris mass balance, and a function that modifies the ice mass balance with respect to the amount of surface debris; the model is solved numerically. The model demonstrates that a debris-covered glacier in steady state must be infinitely long and implies that existing debris-covered glaciers are not in steady state. The terminus of a debris-covered glacier is a critical, dynamic region that must constantly advance. The amount of debris input into the model strongly influences the form of the resultant glacier. A relatively large amount of debris produces a debris-covered glacier with a significant amount of ice beneath the debris, a morphology shared by many ice-cored rock glaciers. Less debris input into the system results in a thicker debris cover on top of a thinner layer of ice. Preliminary model results are consistent with observations from the Galena Creek rock glacier, Wyoming.

NOTATION

$a_d(x)$ = debris mass balance	$Q_d(x)$ = surface debris flux
$a_i(x)$ = ice mass balance	$Q_i(x)$ = ice flux
b = ablation function constant	$v_{av}(x)$ = average longitudinal ice velocity
A = flow law constant	$v_s(x)$ = longitudinal ice velocity at surface
$d(x)$ = depth of debris	$v_x(x,z)$ = longitudinal ice velocity
D = debris mass balance coefficient	$v_z(x,z)$ = surface-normal ice velocity
E = x -coordinate of the ELA	x = distance downglacier
g = gravitational acceleration	z = distance below ice surface
$h(x)$ = depth of ice	θ = surface slope of ice
M = ice mass balance coefficient	ρ_d = density of debris
n = flow law constant	ρ_i = density of ice

INTRODUCTION

This paper develops a simple, steady-state, flow line model of a debris-covered glacier. The objective is to increase understanding of the physical dynamics of these poorly understood glaciers. Although the morphology of debris-covered glaciers is well studied (e.g. Nakawo, 1979; Nakawo *et al.*, 1986; Clark *et al.*, 1994), their flow

dynamics have received little detailed attention. We are motivated in part by our continuing work (Potter, 1972; Steig *et al.*, 1998; Konrad *et al.*, 1999) on the ice-cored Galena Creek rock glacier (GCRG) of the Absaroka Mountains, Wyoming (Fig. 1). Drilling on that glacier (and similar observations from the Murtèl I rock glacier in Switzerland by Haerberli *et al.*, 1988) reveals up to 25 m of continuous ice underneath

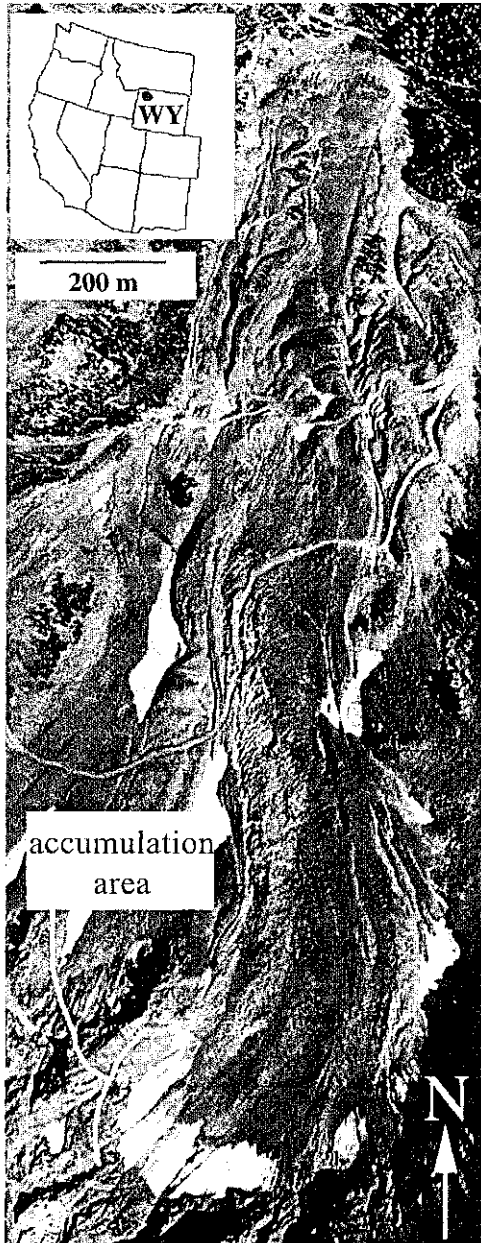


Fig. 1 Aerial photograph of Galena Creek rock glacier (August, 1985). Note relatively small size of the accumulation area.

about a metre of loose surface debris. Although the ice contains entrained debris, including some debris layers, the overall percentage of debris is small (Potter *et al.*, 1998). We assume that the ice will deform with the same stress/strain relationship as glacier ice, and consequently base our model on standard glaciological flow laws.

The flow law assumption implies dynamic similarities between debris-covered glaciers and typical alpine glaciers. However, the surface debris cover complicates the system in two ways: (a) by adding an additional overburden stress, and (b) by inhibiting ablation (if the debris layer is more than several centimetres thick) (Østrem, 1959; Loomis, 1970; Lundstrom *et al.*, 1993). The mass balance patterns of typical alpine glaciers and debris-covered glaciers are distinctly different. The accumulation area comprises about two-thirds of the entire surface area of a steady-state alpine glacier, but much less of a debris-covered glacier (Clark *et al.*, 1994). For example, the accumulation area of GCRG represents only about 10% of the glacier surface (Fig. 1). On a typical, steady-state glacier, annual mass balance decreases with elevation. The mass balance of a debris-covered glacier is strongly influenced by the spatial variation of surface debris. Generally, the surface debris thickens in the downglacier direction (Nakawo, 1979; Konrad *et al.*, 1999), causing the net annual ablation to *decrease* from near the ELA to the terminus, the reverse of the ablation pattern observed on a typical glacier (Fig. 2).

Our model explores the effects of the “reversed” mass balance, and describes the physical behaviour of both debris-covered glaciers and ice-cored rock glaciers, provided that they consist of relatively clean, continuous ice overlain by surface debris. Although lacking many refinements, the model captures the essence of debris-covered glacier dynamics, and will act as a guide to future work.

MODEL

The steady-state flow model is two-dimensional in a vertical section along the centre flow line, with a surface-parallel coordinate system (Fig. 3). The model imposes

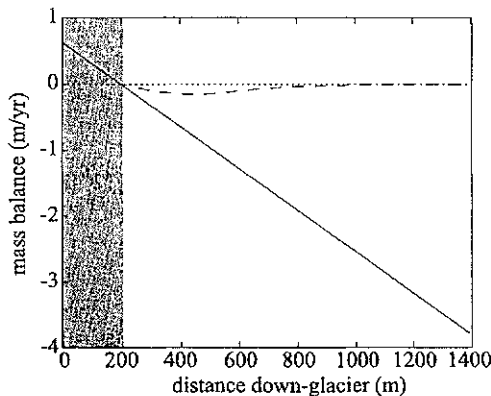


Fig. 2 Ice mass balance of a normal glacier (solid line) compared to a debris-covered glacier (dashed line). Dotted line is zero mass balance. A steady-state debris-free glacier under these conditions is 400 m long, whereas a steady-state debris-covered glacier is infinite in length. The solid line represents the mass balance function without debris, $M = 0.6 \text{ m year}^{-1}$. The dashed line gives the mass balance inclusive of the insulating effects of the debris, a_i . The accumulation area is shaded.

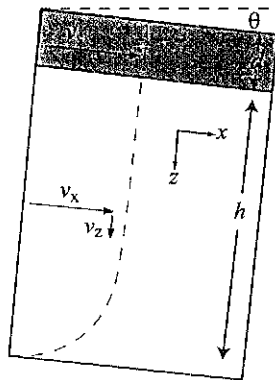


Fig. 3 Schematic illustration of the coordinate system and basic variables of the debris-covered glacier system. x is measured from the top (headwall) of the glacier; z is measured from the ice surface. Surface debris is shaded.

conservation of both ice and debris and uses a simplified force balance based upon the parallel-sided slab ice flow model which ignores effects of ice coupling along the glacier axis or transverse to the flow (Paterson, 1994). The ice deformation at any point depends on the shear stress generated by the downslope component of the overburden weight of ice and debris. Ice coupling transverse to flow is minor if the width of the glacier is much greater than the depth (Nye, 1965). Ignoring longitudinal ice coupling is more problematic since slope, depth, and velocity vary rapidly in the accumulation area; consequently we expect our model to apply poorly in this region. Our model should accurately describe the flow dynamics in the debris-covered region, where gradients in depth and velocity are relatively small. We assume that the surface debris is transported by the underlying ice, with no internal movement of its own (reasonable for low-angle slopes). Additionally, we assume no basal sliding, which is in keeping with observations from GCRG (Konrad *et al.*, 1999).

Our model is a general one, designed to provide insight into the dynamic effects of debris cover on ice. In order to maintain simplicity, we make certain assumptions, such as no basal sliding and restricting the surface debris input to the ELA. We justify the assumptions with observations from GCRG, and note that they may need to be altered in order to fit other debris-covered glaciers. In all cases we choose simple input values (constant or linear in space) and loosely base the numeric choice on observations from GCRG.

Governing functions

Our model is based on conservation of ice and debris; changes in ice or debris flux must be caused by external sources or sinks. The following mass balance equations are based on flux per unit width:

$$\frac{dQ_d}{dx} = \frac{d(dv_s)}{dx} = a_d \quad (1)$$

$$\frac{dQ_i}{dx} = \frac{d(hv_{av})}{dx} = a_i \quad (2)$$

Equation (2) assumes that there is no basal melt or accumulation, as the ice mass balance, a_i , refers to surface processes. Expansion of (2) leads to the differential equation:

$$\frac{dh}{dx} = \frac{a_i}{v_{av}} - \frac{h}{v_{av}} \left(\frac{dv_{av}}{dx} \right) \quad (3)$$

We derive the longitudinal velocity by modifying the parallel-sided flow model to account for the weight of the debris (after Konrad *et al.*, 1999):

$$v_x(z) = \frac{2A(\rho_i g \sin \theta)^n}{(n+1)} \left[\left(h + \frac{\rho_d}{\rho_i} d \right)^{(n+1)} - \left(z + \frac{\rho_d}{\rho_i} d \right)^{(n+1)} \right] \quad (4)$$

Note that $v_s = v_x(0)$. Integration of equation (4) in z gives the average ice velocity:

$$v_{av} = \frac{2A(\rho_i g \sin \theta)^n}{(n+1)(n+2)h} \left[h(n+2) \left(h + \frac{\rho_d}{\rho_i} d \right)^{(n+1)} + \left(\frac{\rho_d}{\rho_i} d \right)^{(n+2)} - \left(h + \frac{\rho_d}{\rho_i} d \right)^{(n+2)} \right] \quad (5)$$

Equations (1) and (3)–(5) form a complete set of four equations and four unknowns (h , d , v_s , v_{av}). We use a second-order Runge-Kutta technique to solve this equation set, starting at the cirque and working downglacier. We use the following values for the constants: $A = 4.0 \times 10^{-24} \text{ s}^{-1} \text{ Pa}^{-3}$ (for -1°C ice, Paterson, 1994), $n = 3$, $\rho_i = 900 \text{ kg m}^{-3}$, $\rho_d = 1800 \text{ kg m}^{-3}$, $g = 9.8 \text{ m}^2 \text{ s}^{-1}$, and use a constant surface slope, $\theta = 15^\circ$, that reflects the average GCRG slope. Note that the model input is the surface slope, as opposed to the unknown bedrock slope. The only input variables are the ice mass balance, a_i , and the debris mass balance, a_d . The model outputs are ice depth, debris depth, and consequently the bedrock profile.

We justify our choice of a constant surface slope in that it reduces the model's complexity, albeit at the expense of poorly modelling the typically steep accumulation area. However, we are primarily interested in the behaviour of the debris-covered ablation area. A more subtle consequence of our assumption is that the glacier bed profile must adjust to contain the steady-state amounts of ice and debris determined by the model. In most models, the surface slope adjusts to fit a specified bedrock profile. We note that when the glacier depth varies rapidly (such as in the accumulation area), the assumption of a constant surface slope generates unlikely bedrock profiles.

As a final step, we generate flow lines and isochrons within the debris-covered glacier. In order to do this, we assume incompressibility of ice to calculate the vertical velocity from (4):

$$v_z = - \int_h^z \frac{\partial v_x}{\partial x} \partial z \quad (6)$$

Boundary conditions

We start the integration at $x = 0$, at the top of the accumulation zone, where we specify $h(0)$ as a finite depth close to zero, and $d(0) = 0$. The ice mass balance is a function

both of elevation (or x in the case of constant surface slope) and of the amount of surface debris. A typical, linear mass balance function that decreases with elevation describes the mass balance without the debris cover. Observations from GCRG suggest that the mass balance is close to zero on the lower rock glacier, where the debris cover is more than several metres deep (Konrad *et al.*, 1999). Higher on the rock glacier, ablation is greater, reaching a maximum slightly downglacier from the accumulation area, in a region of approximately 1 m of surface debris. Operating under the assumption that several metres of debris severely inhibits ablation, but that significant ablation still occurs beneath a metre of debris, we define annual mass balance as:

$$a_i = M \left(1 - \frac{x}{E} \right) \left(e^{-bd} \right) \quad (7)$$

M is the mass balance coefficient, which may be regarded as the ice equivalent of the snow fall/avalanche net contribution at the glacier head, while b is an exponential decay factor describing the insulating effect of debris thickness. Only M varies in our model, with the x -coordinate of the ELA, E , remaining fixed at 200 m, and b at 2 m^{-1} . The linear relationship of a_i to M implies that a reduction in accumulation must be accompanied by a reduction in ablation. We note however, that the ablation rates are largely controlled by debris thickness and not by elevation (Fig. 2). Values of M used in this study vary from 0.6 to 1.2 m year^{-1} .

The ice mass balance function is a schematic approximation: the linear dependence on altitude is only approximate, and the response to the debris cover is an extrapolation of numerous studies (summarized by Clark *et al.*, 1994). Nevertheless, this form of the function captures the “reversed” mass balance pattern observed on debris-covered glaciers in dry environments (Fig. 2). It is probable that this function would be more complex in a wet environment where water can directly advect heat through the debris cover.

The accumulation area of most debris-covered glaciers is primarily debris-free, as debris deposited here will not remain on the surface due to the positive ice mass

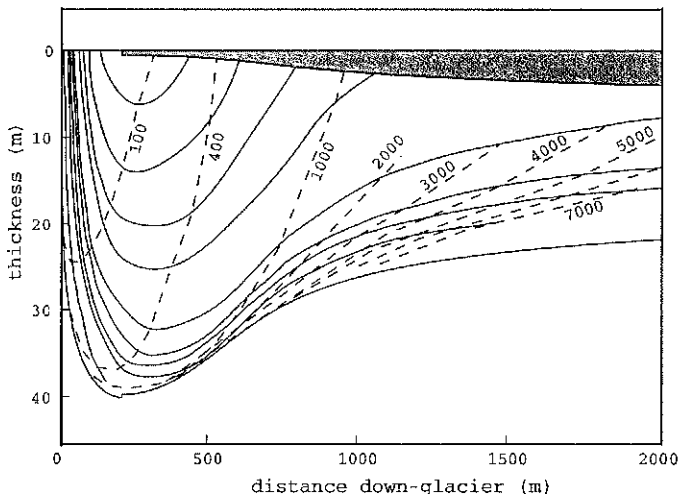


Fig. 4 Typical debris-covered glacier as generated by the model. In this particular case, $M = 0.6 \text{ m year}^{-1}$ and $D = 1.3 \text{ m year}^{-1}$. Flow lines are solid and isochrons are dashed, ages are shown in years. The surface debris is shaded.

balance. Most debris is transported across the accumulation area by avalanche processes, and accumulates on the surface as the slope lessens away from the cirque (Potter, 1972). The downglacier steady-state flux of debris must be constant in both space and time as there are no other significant sources or sinks for rock debris. We represent this debris input pattern as a single point source at the ELA:

$$a_d = D\delta(E) \quad (8)$$

where $\delta(E)$ is the Dirac delta function at $x = E$. D is the debris balance coefficient, and represents the amount of debris added to the system at the ELA. In test runs, we allow D to vary from 1.3 to 2.6 m year⁻¹. An additional possible debris source derives from ice ablation, as any debris within the ice will be added to the bottom of the surface debris layer as the ice melts. At GCRG, it is reasonable to ignore this debris source, as the debris content of the ice is relatively low (Potter *et al.*, 1998). For the purposes of modelling debris-covered glaciers in which a large portion of the debris comes from ice ablation, (8) can be modified to be a function of ablation rates and debris content of the ice (e.g. Nakawo *et al.*, 1986).

RESULTS AND DISCUSSION

A typical debris-covered glacier generated by our model is shown in Fig. 4. Ice is significantly thicker in the accumulation area than in the ablation area, this is in part due to the assumption of constant surface slope. Debris cover gradually thickens down-valley, as the ice depth gradually thins. Within the accumulation area, the ice follows flow lines similar to those of a typical glacier. However, the flow paths in the ablation area are quite different: instead of curving up to meet the surface as in a debris-free glacier, the flow initially curves towards the surface (where ablation rates are relatively high) but turns back to parallel the surface further down-valley (where ablation rates approach zero). Predicted flow velocities are slow (~0.6 m year⁻¹ on the majority of the debris-covered region), resulting in old ice underneath the debris cover. Ice older than ~1000 years is not expected in typical alpine glaciers: our model helps to explain the ice ages of 1600 and 2200 years measured on the upper reaches of GCRG (Konrad *et al.*, 1999).

The most striking result is that the glacier does not have a defined terminus: in steady state, because the debris cover forces the ablation to approach zero, the ice continues to flow down-valley. This is predicted by a comparison of the mass balance functions in Fig. 2. In order for the glacier to be in steady state, the area under the curves in the accumulation area and the ablation area must be equal. In the debris-free case, the steady-state glacier will be 400 m long. Because the area under the curve in the ablation area of the debris-covered glacier is highly bounded, the glacier must be infinite in length for the total ablation to equal the total accumulation.

Effects of varying input mass balances

The form of the resulting debris-covered glacier varies with the specified ice and debris mass balances, controlled by the coefficients M and D , respectively (Fig. 5). A large D and small M cause the majority of the ice mass to be found in the debris-

covered tongue (Fig. 5(c)). For a given M , if D is increased, the result is both a thickening and speeding up of the debris-covered tongue. The maximum glacier depth does not change, but the total amount of ice is greater (compare Fig. 5(a) and (b) with 5(c) and (d), respectively). The increase in D results in a thinner layer of surface debris: this anti-intuitive result is caused by the increased ice velocity. For a given D , an increase of M actually results in less ice, although the maximum depth increases slightly (compare Fig. 5(a) and (c) with 5(b) and (d), respectively). There are two explanations for this: (a) increasing M increases the ice velocity, causing the debris layer to thin and increasing ablation; and (b) an increase of M increases both accumulation in the accumulation area and ablation in the ablation area. In the extreme case of large M and small D (not pictured) we develop a cirque glacier, with a small debris-covered tongue. This approaches the form of a debris-free glacier, for which $D = 0$.

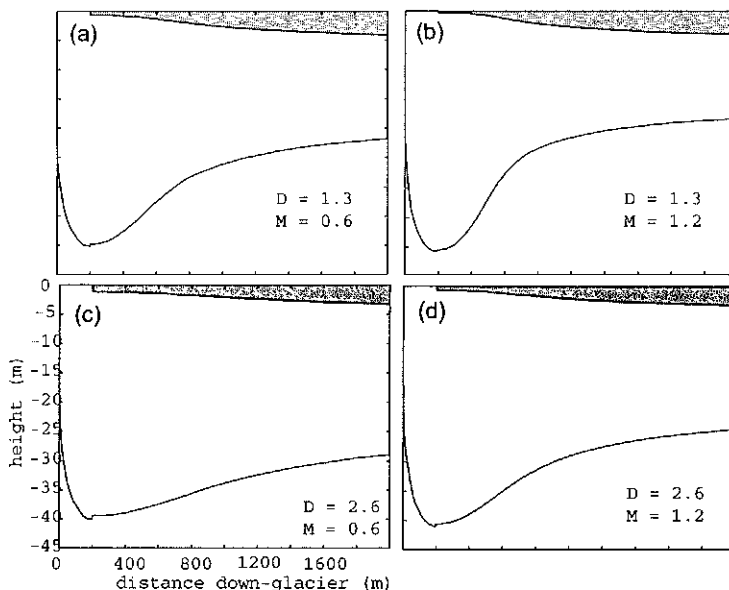


Fig. 5 Variations of glacier geometry with changes in ice mass balance (M , in m year^{-1}) and debris mass balance (D , in m year^{-1}).

Terminus region

Two conclusions immediately result from the observation that a debris-covered glacier cannot be in steady state: (a) the terminus of an active debris-covered glacier must advance, and (b) the length of the debris-covered glacier is some function of its age. Our model leaves the terminus region undefined: downglacier modelling is merely truncated. However, a conceptual examination is worthwhile. Imagine a debris-covered glacier that is not infinitely old and therefore has an advancing terminus located at a finite distance from the headwall. At the terminus, debris rests on top of ice that is now exposed (on the downglacier side) to the air and to ablation. The exposed ice quickly melts, causing the overlying debris to ravel down the face of the glacier, and start accumulating at the base of the ice face. The debris builds up along

the ice face, again insulating it from ablation. However, the ice is still flowing forward, and overrides the fallen debris. The above processes of ablation, debris travelling down the face, and the glacier advancing and overriding debris occur together as a continuous cycle as the terminus advances down-valley. The amount of debris underlying the glacier at any given point is directly related to processes at the terminus at the time at which the debris was overridden (essentially the ratio of longitudinal ice velocity to longitudinal ablation on the ice face). The underlying debris layer can also be thought of as a debris sink, or a way to remove debris from the debris-covered glacier system. We know from drilling at GCRG (Konrad *et al.*, 1999) and Murtèl I (Haeberli *et al.*, 1988) that debris (possibly ice-saturated) underlies the continuous ice layer. We have also observed debris travelling down the steep terminus face of GCRG. Finally, the standard criterion used to identify an active rock glacier (as opposed to stagnant) is an advancing terminus (Wahrhaftig & Cox, 1959). All these observations support our conceptual model of the behaviour of the terminus.

Acknowledgements This research was supported by NSF Grant EAR-9710061, and a National Science Foundation Graduate Student Fellowship.

REFERENCES

- Clark, D. H., Clark, M. M. & Gillespie, A. R. (1994) Debris-covered glaciers in the Sierra Nevada, California, and their implications for snowline reconstructions. *Quatern. Res.* **41**, 139–153.
- Haeberli, W., Huder, J., Keusen, H. R., Pika, J. & Röthlisberger, H. (1988) Core drilling through rock glacier-permafrost. In: *Proceedings of the Fifth International Conference on Permafrost* (Trondheim, Norway) (ed. by Senneset-Kaare), vol. 2, 937–942. International Permafrost Association, Copenhagen, Denmark.
- Konrad, S. K., Humphrey, N. F., Steig, E. J., Clark, D. H., Potter, N. Jr & Pfeffer, W. T. (1999) Rock glacier dynamics and paleoclimatic implications. *Geology* **27**(12), 1131–1134.
- Loomis, S. R. (1970) Morphology and ablation processes on glacier ice. Part I. Morphology and structure of an ice-cored medial moraine, Kaskawulsh Glacier, Yukon. *Arctic Inst. of N. Am. Res. Pap.* **57**, 1–65.
- Lundstrom, S. C., McCafferty, A. E. & Coe, J. A. (1993) Photogrammetric analysis of 1984–89 surface altitude change of the partially debris-covered Eliot Glacier, Mount Hood, Oregon, USA. *Ann. Glaciol.* **17**, 167–170.
- Nakawo, M. (1979) Supraglacial debris of G₂ Glacier in Hidden Valley, Mukut Himal, Nepal. *J. Glaciol.* **22**(87), 273–283.
- Nakawo, M., Iwata, S., Watanabe, O. & Yoshida, M. (1986) Processes which distribute supraglacial debris on the Khumbu Glacier, Nepal Himalaya. *Ann. Glaciol.* **8**, 129–131.
- Nye, J. F. (1965) The flow of a glacier in a channel of rectangular, elliptic or parabolic cross-section. *J. Glaciol.* **5**, 661–690.
- Østrem, G. (1959) Ice melting under a thin layer of moraine, and the existence of ice cores in moraine ridges. *Geogr. Ann.* **41**, 228–230.
- Paterson, W. S. B. (1994) *The Physics of Glaciers*, third edn. Pergamon Press, New York, USA.
- Potter, N. Jr (1972) Ice-cored rock glacier, Galena Creek, Northern Absaroka Mountains, Wyoming. *Geol. Soc. Am. Bull.* **83**, 3025–3058.
- Potter, N. Jr, Steig, E. J., Clark, D. H., Speece, M. A., Clark, G. M. & Updike, A. B. (1998) Galena Creek Rock Glacier revisited—new observations on an old controversy. *Geogr. Ann.* **80A**, 251–266.
- Steig, E. J., Fitzpatrick, J. J., Potter, N. Jr & Clark, D. H. (1998) The geochemical record in rock glaciers. *Geogr. Ann.* **80A**, 277–286.
- Wahrhaftig, C. & Cox, A. (1959) Rock glaciers in the Alaska Range. *Geol. Soc. Am. Bull.* **70**, 383–436.